AENSI Journals

Australian Journal of Basic and Applied Sciences

(ISSN 1991-8178)

Journal home page: www.ajbasweb.com

The possible protective effect of nigella sativa oil on sodium fluoride neurotoxicity in adult male albino rat

[1]Neveen M. El-Sherif, [2]Wael B. El-Kholy

[1]*Affiliation of first author, Anatomy and Embryology department, Faculty of Medicine, Menoufiya University Box.3030 Egypt.*
[2]*Affiliation of second author, Anatomy and Embryology department, Faculty of Medicine, Menoufiya University Box.3030 Egypt.*

ARTICLE INFO

Article history:
Received 20 September 2014
Received in revised form 21 November 2014
Accepted 25 December 2014
Available online 7 February 2015

Keywords:
Sodium fluoride, neurotoxicity, nigella sativa oil, immunohistochemistry.

ABSTRACT

Background: Fluoride has long been recognized as one of the best health measures in the prevention of dental caries. Excessive exposure to fluoride may induce undesirable effects on various body organs. The nigella sativa was reported to have antioxidant and anti-inflammatory properties. **Objectives:** To investigate the possible histological and immunohistochemical changes in the frontal cerebral cortex, dentate gyrus and cerebellum of sodium fluoride (NaF) intoxicated adult male albino rat and evaluate the possible protective role of nigella sativa oil (NSO). **Materials and methods:** Twenty adult male albino rats weighing 150–200g were randomly divided into four equal groups: control, NSO treated (2 ml/kg/day), NaF treated (20 mg/kg /day) and protected (NaF+NSO). At the end of experiment (4 weeks) the frontal cerebral cortex, dentate gyrus and cerebellum were processed for light microscopic examination. Quantitative immunohistochemical assessment and statistical analysis of the expression of inducible NO synthase (iNOS), Bax protein, Bcl-2 protein, tumor necrosis factor (TNF)-α and glial fibrillary acidic protein (GFAP) were performed. **Results:** Our results revealed the protective role of NSO on NaF neurotoxicity via reducing oxidative stress, apoptosis and inflammation. In addition, this study revealed that the beneficial effect of NSO was also mediated by modulating the astroglial response to the injury. **Conclusion:** Chronic exposure to sodium fluoride results in neurotoxicity. Furthermore, combined nigella sativa oil supplementation has an ameliorating effect on these changes.

To Cite This Article: Neveen M. El-Sherif, Wael B. El-Kholy, The possible protective effect of nigella sativa oil on sodium fluoride neurotoxicity in adult male albino rat. ***Aust. J. Basic & Appl. Sci.,*** *9(2):346-361, 2015*

INTRODUCTION

Fluoride is an essential trace element from the halogen group that has protective effects against bone mineral loss. Also, it can prevent caries and enamel fluorosis. Sodium fluoride is commonly added to drinking water, tooth pastes and some mouth washes as decay preventive ingredient (Chouhan and Flora, 2010). Consumption of 1mg fluoride per day is essential for humans as fluoride is safe and effective when consumed properly (Jha *et al*., 2013). If fluoride is consumed in high quantities, it can cause severe damage to most tissues including primarily the dental and skeletal systems (Ricomini Filho *et al*., 2012). Experimental studies exhibited that fluoride accumulation was observed in the brain of experimental animals exposed to chronic fluoride intake and this accumulation increased as drinking water fluoride content increased (Mullenix *et al*., 2005). Previous studies have shown that rats drinking only 1 part per million fluoride in water had histological lesions in their brain similar to Alzheimer's disease and dementia. In addition, evidence pointed to possible damage to the blood–brain barrier from prolonged exposure to fluoride (Graves *et al*., 2009). It was reported that long term intake of high level of fluoride in human caused neurological complications such as paralysis of limbs, vertigo, spasticity in extremities and impaired mental acuity (Lu *et al*., 2000). Moreover, other investigators found that water fluoride greater than certain level adversely affects the development of children's intelligence (Xiang *et al*., 2003). Chronic fluoride toxicity is also found to cause altered neuronal and cerebrovascular integrity, abnormal behavior patterns and metabolic lesions in the brain of experimental animals (Vani and Reddy, 2000). Moreover, other studies stated that chronic exposure of pregnant and lactating mothers to high level of fluoride affect some biochemical indexes of the brain and learning memory abilities of their offsprig's (Wang *et al*., 2004). Generation of free radicals, lipid peroxidation and altered anti-oxidant defense system are considered to play an important role in toxic effect of fluoride (Dhar and Bhatnagar, 2009).

The frontal cerebral cortex comprises most of motor areas and important vital centers. It is considered to be responsible for programming of complex motor activities (Sofroniew andVinters, 2010).

Corresponding Author: Neveen M. El-Sherif, Anatomy and Embryology department, Faculty of Medicine, Menoufiya University Box.3030 Egypt.

The hippocampus is a major component in the brains of humans and other vertebrates. It is a part of the limbic system and plays important roles in the consolidation of information from short-term memory to long-term and spatial memory. It contains two main interlocking parts: Ammon's horn and the dentate gyrus. The hippocampus has been reported to be sensitive to neurotoxic insults and is one of the first regions of the brain to suffer damage (Nolte, 2009(. The dentate gyrus, which constitutes a part of the hippocampus, is thought to contribute to the formation of new memories (Saab *et al*., 2009).

The cerebellum plays an important role in movement and posture. Malformation and lesions of the cerebellum disrupt motor coordination and impair balance. The cerebellum is also involved in a variety of non-motor cognitive functions, including sensory discrimination, attention, learning, and memory (Northam and Cameron, 2013).

Nigella sativa is a plant known to have antioxidant properties and its main component (constituting 30–48%) is thymoquinone, which has many therapeutic effects (Nagi *et al*., 2010). The seeds of N. sativa are used extensively in the traditional medicine of many countries (Meddah *et al*., 2009). Its oil extract (N. sativa oil; NSO) is most often used medicinally for its protective role against many diseases owing to the reported anti-inflammatory (Hajhashemi *et al*., 2004), antidiabetic (Kanter *et al*., 2004), and hepatoprotective activities (El-Gharieb *et al*., 2010).

Previous literature regarding, detailed histological changes in fluoride-induced neurotoxicity is lacking. However, very few studies have dealt with its possible protective role of NSO against NaF induced neurotoxicity. Thus the present study was aimed to investigate the possible histological and immunohistochemical changes in the frontal cerebral cortex, dentate gyrus and cerebellum of NaF intoxicated rat and evaluate the possible protective role of NSO in adult male albino rat.

MATERIALS AND METHODS

Animals:

Twenty adult male albino rats aged 10-12 weeks at an average weight 150–200g were used in this study. Each group was kept in a separate cage under good hygienic conditions, fed ad libitum, and allowed free access to water in the animal house of the Faculty of Medicine, Menoufiya University. The rats were treated in accordance with the guidelines approved by the Animal care and Use Committee of Faculty of Medicine, Menoufiya University.

Chemicals:

(1) Sodium fluoride (NaF) was purchased from El-Gomhoria Company (Cairo, Egypt). It was provided in a white powder form.

(2) Nigella sativa oil (NSO) was purchased from the Kahira Pharmaceutical and Chemical Industries Co. (El -Safa, Cairo, Egypt) as 100% pure NSO.

(3) Polyclonal rabbit anti-iNOS (LabVision Corporation, Neomarkers laboratories, CA, USA). Working dilution 1:500.

(4) Monoclonal antibody against Bax protein (Dako, Carpinteria, California, USA). Working dilution 1:500.

(5) Monoclonal anti-Bcl-2 protein (Dako, Carpinteria, California, USA). Working dilution 1:500.

(6) Polyclonal rabbit anti-TNF-α antibody. (Lab Vision Corporation, Neomarkers laboratories, CA, USA). Working dilution 1:1000.

(7) Polyclonal goat anti-GFAP antibody (Lab Vision Corporation, Neomarkers laboratories, CA, USA). Working dilution 1:300.

Experimental Design:

Animals were equally subdivided into four groups:

- **Group I** (Control) each rat was given the same amount of vehicle (distilled water) daily orally for 4 weeks. The required dose for each rat was introduced into the mouth using a syringe with a metal tube instead of a needle.
- **Group II** (NSO treated) received NSO once daily at a dose of 2 ml/kg orally once for 4 weeks. The dose of NSO was chosen to be effective with no adverse effects as reported by (Uz *et al*., 2008).
- **Group III** (NaF treated) each received 20 mg/kg of NaF orally once daily for 4 weeks (Vani and Reddy. 2000). Sodium fluoride solution was prepared by dissolving 1 gm sodium fluoride in 250 ml distilled water so each 1 ml would have 4 mg sodium fluoride. Each rat was given daily 0.75-1 ml of this solution according to its weight.
- **Group IV** (protected) received NSO 30 minutes before oral administration of NaF at the same dose and duration as the previous two groups.

Histological and Immunohistochemical Studies:

At the end of each time point studied, each rat was deeply anaesthetized using ether inhalation. After the chest wall was opened, animals were perfused transcardially through the left ventricle with 10% formol saline. Before perfusion, the descending aorta was ligated and the right atrium was opened once perfusion has started. The perfusion was stopped when the venous return from the right atrium became clear (Venkataraman *et al*., 2010). The skull was opened and the brain was removed. Each brain was fixed in 10% neutral buffered formalin and embedded in paraffin wax for histological examination. Semi-serial 5µm coronal sections (1-in-20 series) were prepared from the frontal cortex, hippocampus, and cerebellar cortex and were dehydrated using ethanol and stained with hematoxylin & eosin (H&E). For immunohistological staining, paraffin sections (5 µm thick) were deparaffinized in xylene for 1–2 min and then rehydrated in descending grades of ethanol (100%, 95%, and 70% ethanol) two changes 5 min each, then brought to distilled water for another 5 min. Sections were rinsed with PBS, blocked for 30 min in 0.1% H2O2 as inhibitor for endogenous peroxidase activity. After rinsing in PBS, sections were incubated for 60 min in blocking solution (10% normal goat serum) at room temperature. The sections were then incubated with the primary antibody (iNOS 1:500; Bax-protein 1:500; Bcl-2 protein 1:500; TNF-α 1:1000 and GFAP 1:300) at room temperature for an hour. Sections were rinsed with PBS, followed by 20 min of incubation at room temperature with secondary biotinylated antibody. After rinsing the sections in PBS, enzyme conjugate "Streptavidin-Horseradish peroxidase" solution was applied to the sections for 10 min. Secondary antibody binding was visualized using 3,3′-diaminobenzoic acid (DAB) dissolved in PBS with the addition of H2O2 to a concentration of 0.03% immediately before use. Finally, sections were PBS rinsed and counterstaining of slides was done using two drops of hemotoxylin. Slides were washed in distilled water until the sections turned blue. Finally, slides were dehydrated in ascending grades of ethanol (70%, 95%, and 100%) for 5 min each and were cleared in xylene and finally coverslipped using histomount mounting solution.

Quantitative Assessment and Statistical Analysis:

Five non-overlapping fields (400×) per section were randomly captured by a digital camera (Olympus) in the frontal cortex and the cerebellum, whereas the entire dentate gyral area was analyzed for each brain section for each marker. The number of immunopositive cells in the fields taken from five anatomically comparable sections/animal was counted using imageJ software and averaged per field for each animal. The numbers calculated for at least five animals/experimental group were considered for comparison and statistical analyses. The statistical analysis for each experimental parameter was performed using the arithmetic mean, standard deviation (X±SD), and analysis of variance (ANOVA). This was followed by Tukey's test for multiple comparisons. P values less than 0.05 were considered significant.

Results:

There was no significant difference between Group I (control) and Group II (NSO treated) rats in all the outcomes at each time point used in the study; therefore, these two groups were pooled in one group (control).

Effect of NSO on the frontal cerebral cortex of NaF neurotoxicity:

H&E stained sections showed that, the frontal cortex of the control group was covered by pia mater and stratified into six layers containing scattered nuclei of both neurons and glial cells. These layers were identified as the outer molecular layer (I), external granular layer (II), external pyramidal layer (III), internal granular layer (IV), internal pyramidal layer (V), and polymorphic layer (VI) (Fig. 1). Neurons of the frontal cortex were of varying shapes and sizes, but the most obvious were the pyramidal cells. Each pyramidal cell in the external pyramidal layer appeared triangular in shape with a basophilic cytoplasm and a centrally located large rounded vesicular nucleus. The smaller neuroglia cells with dense nuclei and numerous granular cells (rounded in shape with large open face nuclei and prominent nucleoli) were scattered in the neuropil (eosinophilic background formed of neuronal and glial cell processes). Blood capillaries were scattered among neurons (Fig. 2).

Examination of H&E stained sections of the frontal cortex of NaF treated rats showed that most neurons were distorted in shape with deeply stained nuclei and surrounded by vacuolated pale areas most probably apoptotic cells. Homogenous acidophilic masses with small fragmented nuclei and surrounded by clear halos were detected. Neuropil showed vascular dilatation. Some cells appeared normal (Fig. 3).

Examination of H&E stained sections of the frontal cortex of protected group revealed that most of nerve cells appeared normal, while few cells appeared distorted with shrunken cytoplasm and deeply stained nuclei. Dilated blood vessels were also observed in this group (Fig. 4).

Quantitative immunohistochemical assessment and statistical analysis was performed (Fig. 5, Histogram 1) A significant up-regulation of iNOS expression, a marker of oxidative distress was detected in the NaF treated group compared with control group (8.09±1.28 vs 00±00). In the protected group, iNOS expression was significantly down-regulated compared with NaF treated rats (2.28±3.34). The elevated expression of iNOS was associated with a significant increase in the number of Bax-protein positive cells in the NaF treated group

compared with controls (12.65±6.24 vs 0.3±0.17), which was significantly reduced in the protected group (2.18±0.56). There was a significant decrease in Bcl-2 protein activity in NaF treated rats compared with control rats (14.65±3.01 vs 52.07±2.31). Interestingly, in the protected group, the decreased Bcl-2 protein expression was significantly increased in the cytoplasm of many nerve cells and endothelial cells of blood vessels (26.01±3.49). The expression of the inflammatory marker TNF-α was significantly increased in the NaF treated group compared with control (7.07±0.37 vs 00±00), this increase showed significant decrease in the protected group (4.68±1.19). In NaF treated brains, the frontal cortex showed a significant increase in GFAP-positive cells (cytoplasm of astrocytes) compared with control (29.13±0.28 vs 10.56±1.18), this increase was significantly decreased in NaF + NSO treated (protected) brains (22.05±5.28).

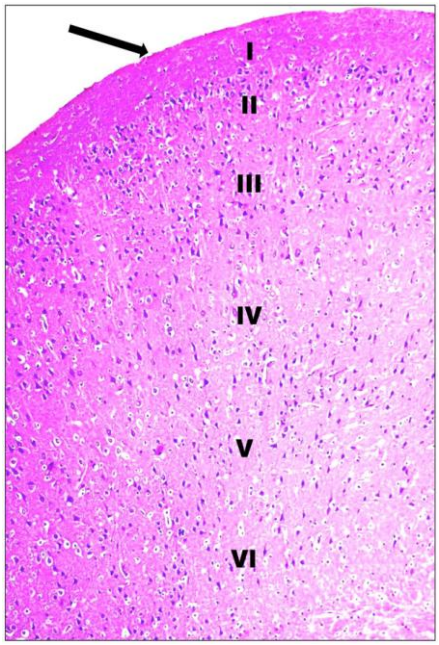

Fig. 1: A photomicrograph of a section in the frontal cortex of a control rat showing the motor cortex covered by pia mater (→). The six layers of the frontal cortex can be identified: outer molecular layer (I), external granular layer (II), external pyramidal layer (III), internal granular layer (IV), internal pyramidal layer (V), and polymorphic layer (VI). H&E, × 100.

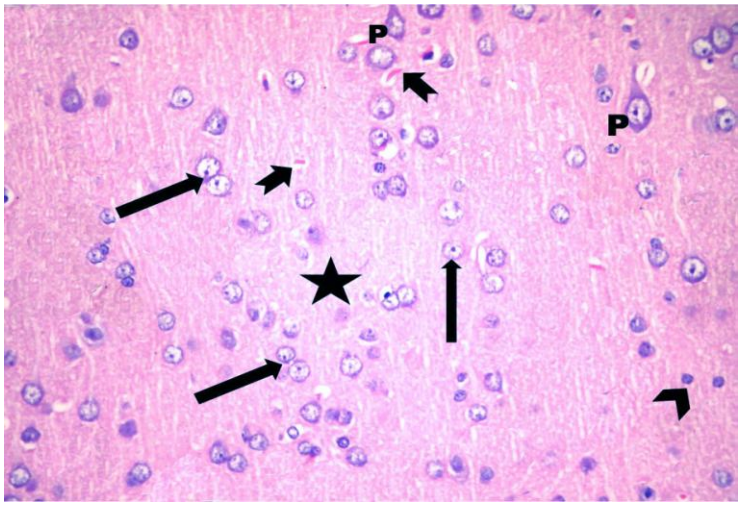

Fig. 2: A photomicrograph of a section in layer III of the frontal cortex of a control rat showing pyramidal cells (P) with large rounded vesicular nuclei, basophilic cytoplasm, and processes. Note the neuroglia cells with small dense nuclei (arrow head) and granular cells with open face vesicular nuclei and prominent nucleoli (→) in the eosinophilic neuropil that forms the background for the cells (*). Blood capillaries (notched arrow) are seen among neurons. H&E, × 400.

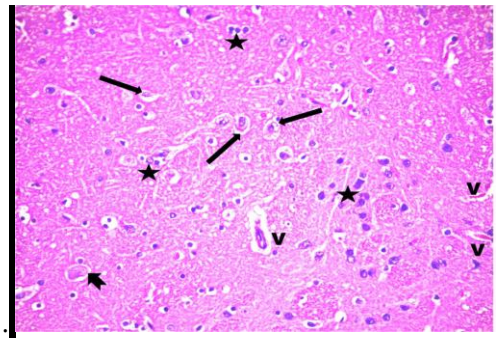

Fig. 3: A photomicrograph of a section in layer III of the frontal cortex of NaF treated rat showing that most cells are distorted with deeply stained nuclei (*). Some cells are surrounded by clear halos (arrow). Homogenous acidophilic masses containing fragmented nuclei and surrounded by halos (notched arrow) are clearly seen. Notice the vascular dilatation (V) in the neuropil. H & E, × 400.

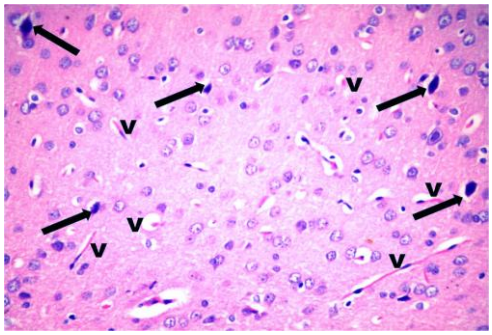

Fig. 4: A photomicrograph of a section in layer III of the frontal cortex of protected group showing that multiple cells appear normal. Few cells appear distorted and shrunken with deeply stained nuclei (arrow). Note the dilated blood vessels (V). H & E, × 400.

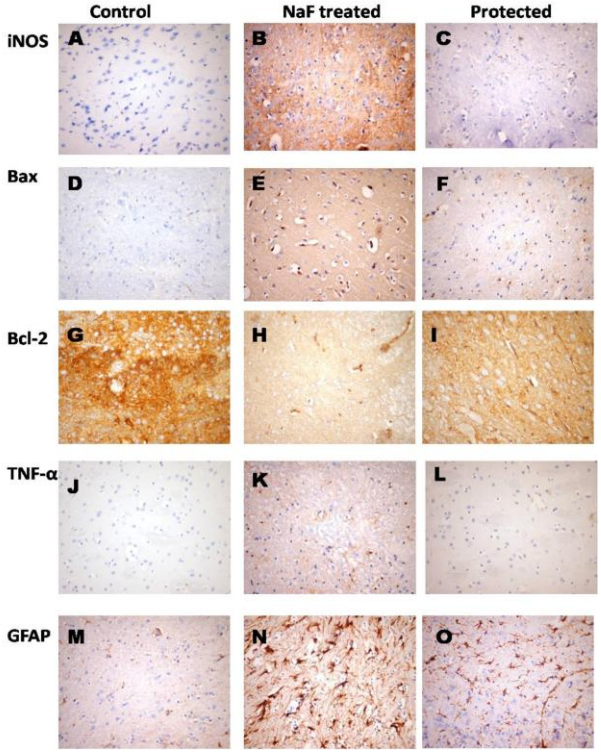

Fig. 5: A photomicrograph of immunostaining sections in the frontal cerebral cortex of different experimental groups showing that, iNOS and Bax-protein immunoreactive cells were increased in NaF treated frontal cortex (B and E). These increases were reduced in the protected group (C and F). Bcl-2 protein immunoreactive cells were decreased in NaF treated frontal cortex (H). These increases were reduced in the protected group (I). NSO treatment attenuated the NaF-induced increase in TNF-α (J–L), GFAP expression (M–O). Immunoperoxidase technique, × 400.

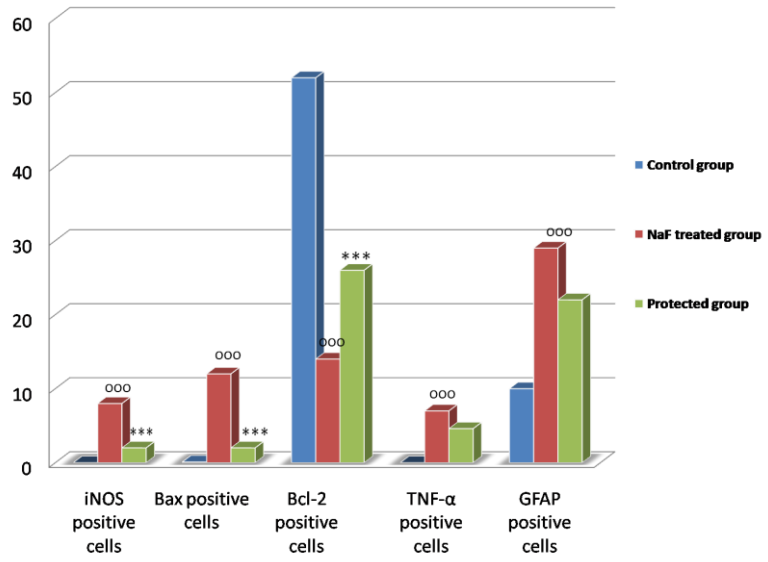

Histogram 1: Representative immunostaining of rat frontal cortex of different groups. * (P <0.05) and *** (P < 0.001) compared with the NaF treated group; 000 (P < 0.001) compared with control.

Effect of NSO on the dentate gyrus of NaF neurotoxicity:

H&E-stained sections of the temporal lobe of the control group showed the hippocampus as a pair of interlocking C-shaped structures: Ammon's horn and the dentate gyrus (Fig. 6). The dentate gyrus was formed of three layers: the molecular, granular and polymorphic layers. The molecular layer was located adjacent to the hippocampus, whereas the granular layer is the most prominent layer composed of densely packed granular cells arranged in V-shaped configuration forming upper and lower blades (Fig. 7). The granule cells of the granular layer appeared with rounded pale vesicular nuclei. The polymorphic layer consisted of pyramidal neurons that appeared as large cells with long processes as well as astrocytes and microglial cells (Fig. 8).

Examination of H&E stained sections of NaF treated group showed dentate gyrus with dilatation and congestion of blood capillaries. The granular cell layer revealed degeneration of most of the granular cells, together with appearance of halos around the shrunken cells. Pyramidal cells of polymorphic layer appeared shrunken with darkly stained pyknotic nuclei (Fig. 9).

In protected group, H&E stained sections revealed that most of the granular neurons appeared normal with rounded vesicular basophilic nuclei. Few pyramidal cells of polymorphic layer appeared distorted with loss of nuclear details. Dilated and congested blood capillaries were still seen (Fig. 10).

Quantitative immunohistochemical assessment and statistical analysis (Fig. 11, Histogram 2) revealed that: iNOS and Bax-protein immunoreactivity, markers of oxidative stress and apoptosis respectively, were increased in the granular layer of the NaF treated dentate gyrus compared with control group (9.18±1.21 vs 00±00), (12.89±2.3 vs 0.7±1.27) respectively. This increase was significantly decreased in the protected group compared with NaF treated rats (2.03±6.26), (3.3±7.56) respectively. Bcl-2 immunostaining revealed a dramatic decrease in the number of positive cells among granular cells (3.07±2.81 vs 48.07±1.53). This down-regulation in the Bcl-2 positive cells was reversed significantly in the protected group in which Bcl-2 positive Immunostained cells was significantly increased (26.09±6.26). The expression of the inflammatory marker, TNF-α, was increased in the NaF treated group compared with control (4.27±7.36 vs 1.46±1.13), this increase showed a significant decrease in the protected rats (2.71±4.26). Dentate gyri of NaF treated brains showed a significant increase in the number of GFAP positive cells especially in the polymorphic layer and to a less extend in the molecular layer as compared with control (58.31±0.32 vs 19.63±1.12). In the protected group, this number was significantly decreased (47.8±3.54).

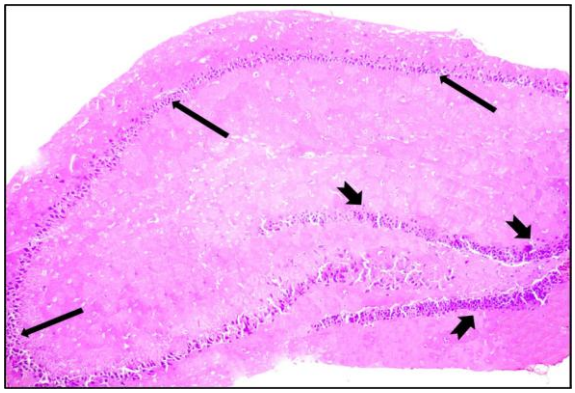

Fig. 6: A photomicrograph of a section of the temporal lobe. The hippocampus appearing as a pair of interlocking C-shaped structures: Ammon's horn (arrow) and the dentate gyrus (notched arrow). H&E, × 100**.**

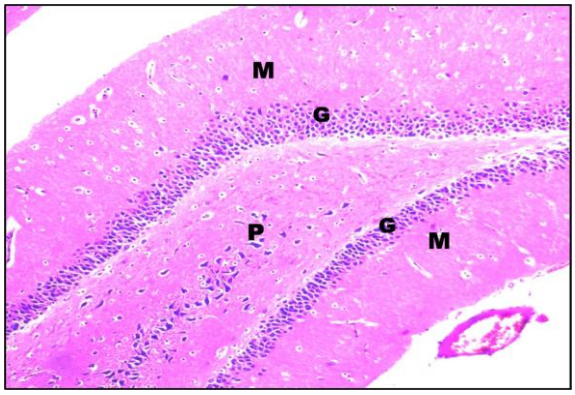

Fig. 7: A photomicrograph of section in the dentate gyrus showing that, dentate gyrus consisting of a molecular layer (M), a granular cell layer (G), and a polymorphic layer (P). H&E, × 200.

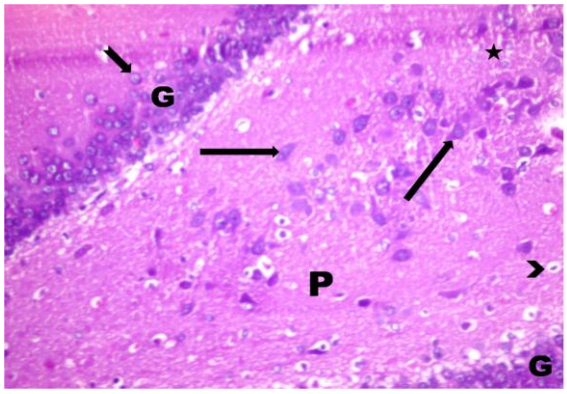

Fig. 8: A photomicrograph of a section in the dentate gyrus of a control rat. The granular cell layer (G) containing granular cells with rounded pale vesicular nuclei (notched arrow). The polymorphic layer (P) containing pyramidal cells with long processes (arrow), astrocytes (*) and microglia (arrow head) is clearly seen. H&E, × 400.

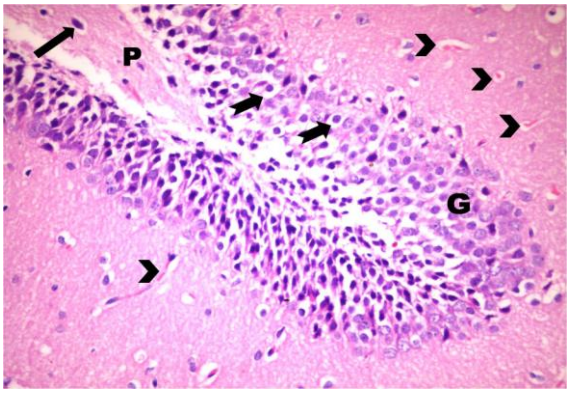

Fig. 9: A photomicrograph of a section in the dentate gyrus of NaF treated rat showing distortion of the granular cell layer G) with halos around shrunken granular cells (notched arrow). Polymorphic layer (P) shows shrunken pyramidal cells (arrow) with darkly stained pyknotic nuclei. Notice the dilated congested blood capillaries (arrow head). H&E, × 400.

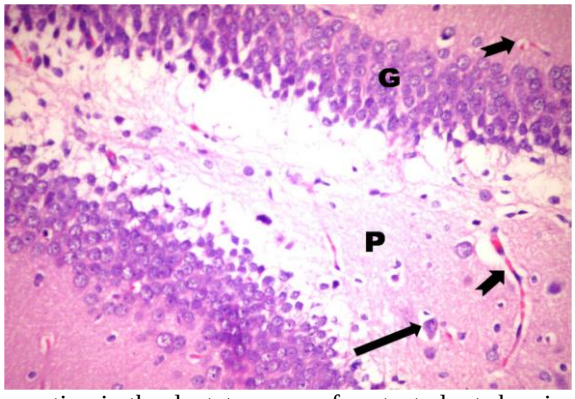

Fig. 10: A photomicrograph of a section in the dentate gyrus of protected rat showing that the granular cell layer (G) appears similar to that of control group. Few pyramidal nerve cells of polymorphic layer (P) appear distorted with loss of nuclear details (arrow). Some dilated congested blood capillaries (notched arrow) can be seen. H&E, × 400

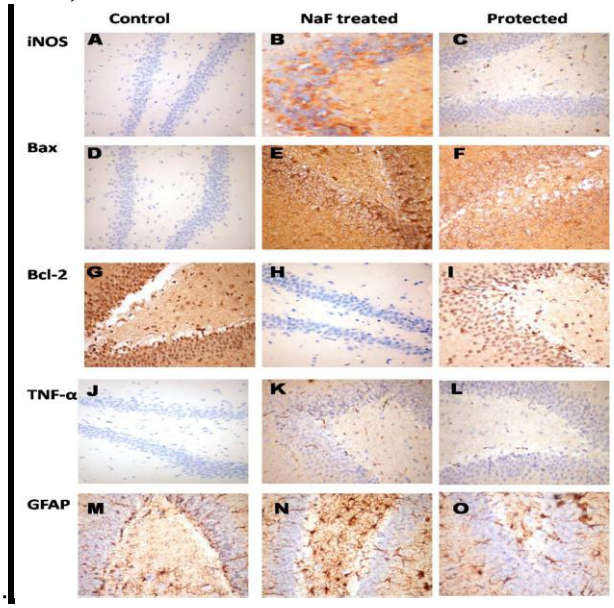

Fig. 11: A photomicrograph of immunostaining sections in the dentate gyri of different experimental groups showing that, iNOS and Bax-protein immunoreactivity were increased in NaF treated dentate gyri (B and E). These increases were reduced in the protected group (C and F). Bcl-2 immunoreactivity was decreased in NaF treated dentate gyri (H). These increases were reduced in the protected group (I). NSO treatment attenuated the NaF-induced increase in TNF-α (J–L), GFAP expression (M–O). Immunoperoxidase technique, × 400.

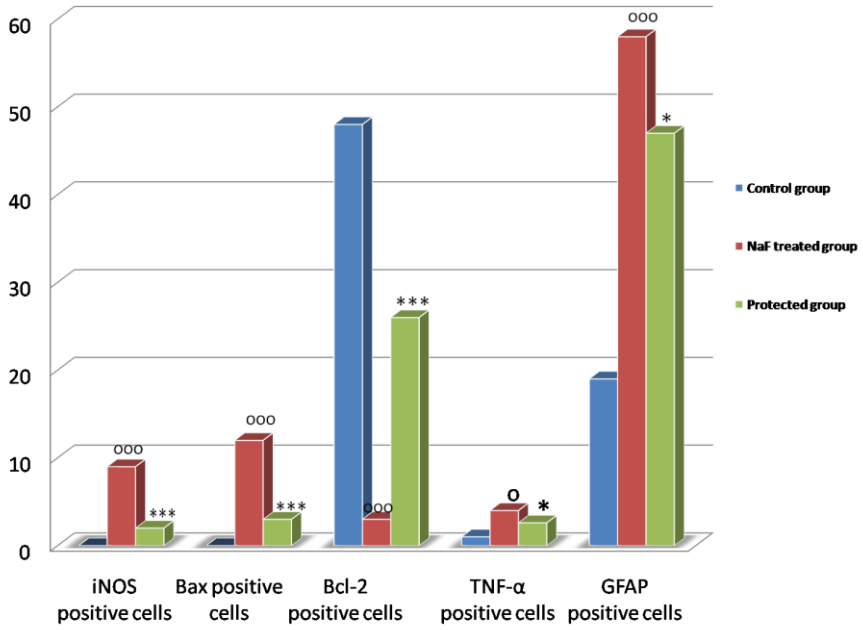

Histogram 2: Representative immunostaining of rat dentate gyri of different groups. * (P <0.05) and *** (P < 0.001) compared with the NaF treated group; 0 (P <0.05) and 000 (P < 0.001) compared with control.

Effect of NSO on the cerebellar cortex of NaF neurotoxicity:

H&E stained sections of control adult rats showed the usual architecture of the cerebellum with folia separated by sulci. Each folium consisted of a mantle of cerebellar cortex and a core of white matter (Fig. 12). The cerebellar cortex was made up of molecular, Purkinje cell and granular layers (Figs13, 14). The molecular layer was formed of glial cells (small stellate and basket cells) together with numerous fibers. Stellate cells were located superficially in this layer, whereas basket cells were found in the deeper parts near Purkinje cell bodies. The Purkinje cell layer was seen arranged in one row along the outer margin of the granular layer. It consisted of a single row of large pyriform somata of Purkinje neurons with clear vesicular nuclei. The granular layer was composed of tightly packed small rounded cells with deeply stained nuclei (Fig. 14).

In NaF treated group, Purkinje cells were the most affected cells that showed irregularity in size and shape with darkly stained nuclei and cytoplasm. Prominent perineuronal spaces were also observed. Some areas showed loss of most Purkinje neurons leaving empty spaces. Congested dilated blood vessel surrounded by a wide perivascular space can be seen in the white matter (Fig 15).

Light microscopic examination of the cerebellar cortex of protected group displayed nearly normal appearance of the molecular, granular, and Purkinje cell layers. Compared with the control group, the Purkinje cells seemed smaller in size. Some cells were shrunked and surrounded by clear perineural spaces (Fig 16).

Quantitative immunohistochemical assessment and statistical analysis (Fig. 17, Histogram 3) revealed that: immunohistochemical staining for iNOS and Bax-protein revealed a significant increase in their number of NaF treated cerebellar cortex (19.88±0.27 vs 1.18±0.07), (19.37±6.23) respectively; this increase was significantly reduced in protected group (11.27±0.24), (2.1±1.77) respectively. Bcl-2 immunostaining revealed a significant decrease in the number of positive cells among granular cells (4.65±4.34 vs 32.07±1.28). This down-regulation in the Bcl-2 positive cells was reversed significantly in the protected group in which Bcl-2 positive Immunostained cells was significantly increased (11.27±6.39). The expression of TNF-α was significantly increased in the cerebellum of NaF treated group (9.16±2.91 vs 2.01±0.08). NSO treatment also reduced NaF induced inflammation as suggested by the significant down-regulation of TNF-α in protected group compared with NaF treated ones (3.29±3.44). The number of cells expressing GFAP was dramatically increased in NaF treated group (70.35±3.74 vs 20.11±2.23). This increase was significantly decreased in protected rats (38.17±0.18).

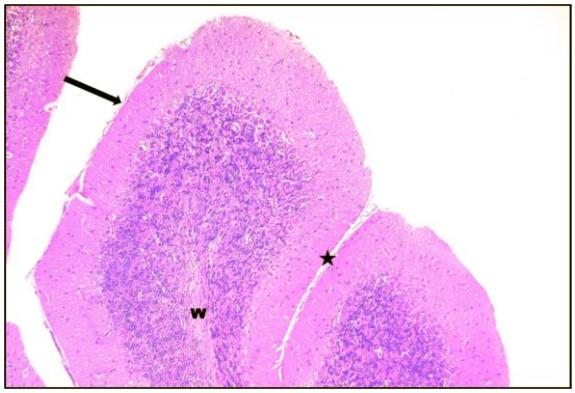

Fig. 12: A photomicrograph of a section in the cerebellum of a control rat showing folia, separated by sulci (*). Each folium consists of a mantle of cerebellar cortex with a core of white matter (W). The covering pia mater can be observed (arrow). H&E, × 100

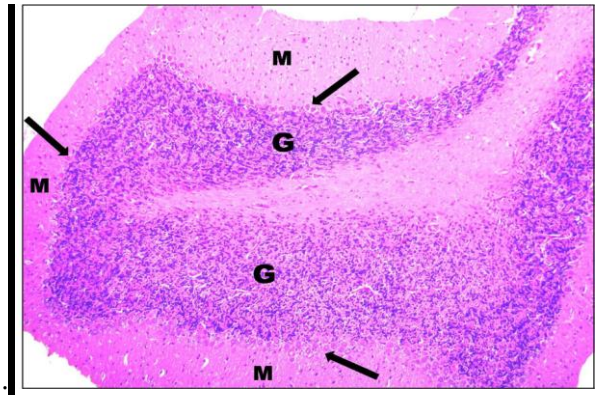

Fig. 13: A photomicrograph of a section in the cerebellar cortex of a control rat exhibiting that it is made up of molecular layer (M), Purkinje cell layer (arrow) and granular layer (G). H&E, × 200.

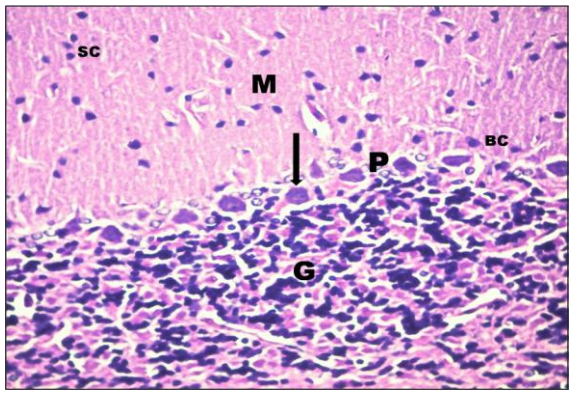

Fig. 14: A photomicrograph of a section in the cerebellar cortex of a control rat displaying molecular layer (M) formed of small stellate (SC) and basket cells (BC) together with numerous fibers. Purkinje cell layer (P) consists of large pyriform cells with vesicular nuclei (arrow), whereas the granular layer (G) is composed of tightly packed small rounded cells with deeply stained nuclei. H&E, × 400.

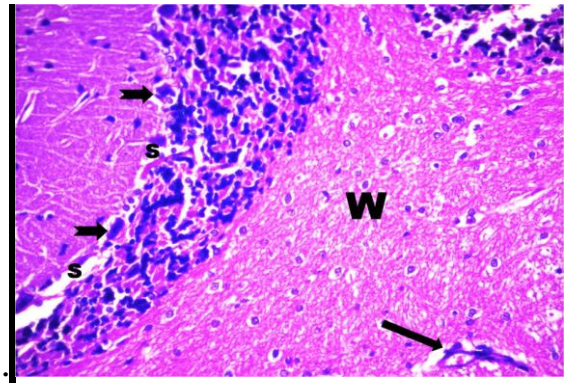

Fig. 15: A photomicrograph of a section in the cerebella cortex of NaF treated rat showing loss of most Purkinje neurons leaving empty spaces (S). Some Purkinje cells appear irregular in size and shape with darkly stained nuclei and cytoplasm with prominent perineuronal spaces (notched arrow). Congested dilated blood vessel surrounded by a wide perivascular space (arrow) can be seen in the white matter (W). H&E, × 400.

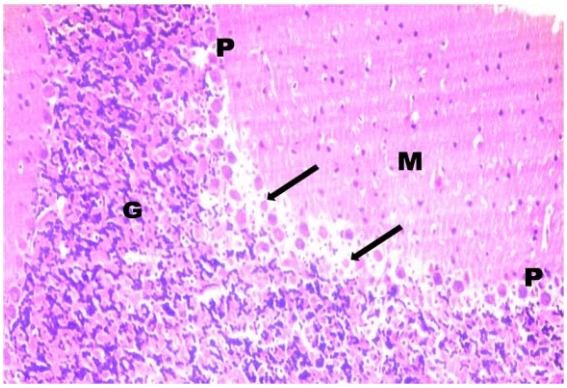

Fig. 16: A photomicrograph of a section in the cerebellar cortex of protected rat exhibiting nearly the sound appearance of the molecular (M), granular (G), and the Purkinje cell layers (P). Some Purkinje cells (arrow) are shrunked and surrounded by perineural spaces. H&E, × 400.

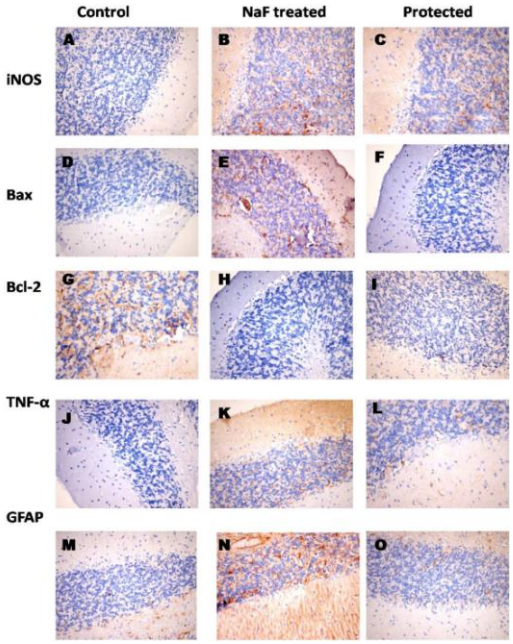

Fig. 17: A photomicrograph of immunostaining sections in the cerebellar cortex of different experimental groups showing that, iNOS and Bax-protein immunoreactivity were increased in NaF treated cerebellar cortex (B and E). These increases were reduced in the protected group (C and F). Bcl-2 immunoreactivity was decreased in NaF treated cerebellar cortex (H). These increases were reduced in the protected group (I). NSO treatment attenuated the NaF-induced increase in TNF-α (J–L), GFAP expression (M–O). Immunoperoxidase technique, × 400.

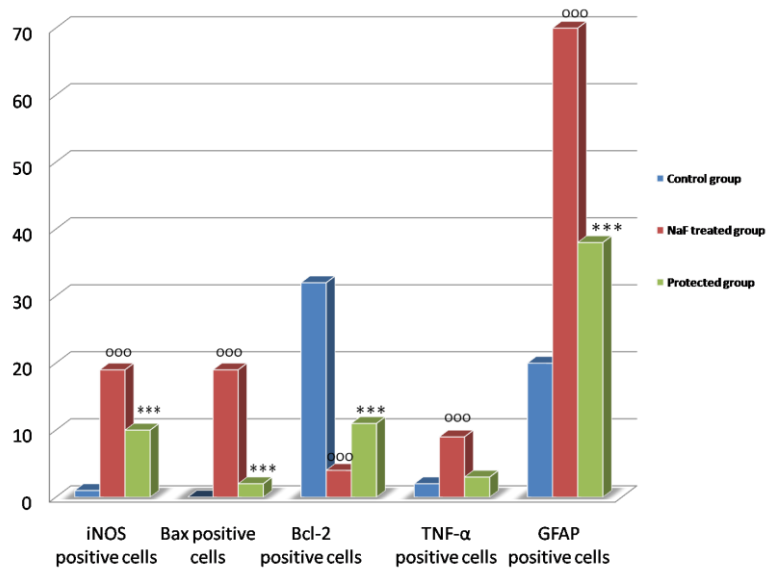

Histogram 3: Representative immunostaining of rat cerebellar cortex of different groups. *** ($P < 0.001$) compared with the NaF treated group; 000 ($P < 0.001$) compared with control.

Discussion:

Fluoride is one of the potential environmental toxicants to which humans are exposed mainly through drinking water (Santoyo-Sanchez *et al*., 2013). Evidence that fluoride crossed the blood brain barrier raised the possibility that fluoride could affect the structure and function of the central or peripheral nervous system (Graves *et al*., 2009) and (Feng *et al*., 2012). The brain is particularly susceptible to oxidative damage due to its high levels of oxygen consumption, increased levels of polyunsaturated fatty acid, and relatively low levels of antioxidants (Flora *et al*., 2012).

The chosen route in this study for exposure was through drinking water to mimic human exposure (Dabrowaska *et al*., 2006).

The results of this work revealed observable alterations in the structure of the frontal cortex of NaF treated rats. Most nerve cells in the cortical layers were distorted in shape with deeply stained shrunked nuclei and cytoplasm and were surrounded by vacuolated pale areas most probably apoptotic cells. Homogenous acidophilic masses surrounded by clear halos were detected. Vascular dilatation was also detected. These results were in agreement with the results obtained by other study which documented that there are distinct morphological alterations in the brain including effects on neurons and the cerebrovascular integrity after chronic administrations of sodium fluoride or aluminum fluoride (Varner *et al*., 1998).

In the current study, examination of the dentate gyrus of the NaF treated group revealed that, the granular cell layer showed degeneration of most of the granular cells, together with appearance of halos around the shrunken cells. Pyramidal cells of polymorphic layer appeared shrunken with darkly stained pyknotic nuclei. Dilated and congested blood capillaries were also observed. These brain changes may be attributed to oxidative damage. The findings of the present research were supported by other reports (Zhang *et al*., 2013) that mentioned that NaF neurotoxicity is characterized by progressive pathological changes in the brain that translate into clinical signs. These changes include deterioration and loss of neurons, leading to brain atrophy or shrinkage with progressive cognitive and behavioral decline.

The NaF treated group showed observable alterations in the structure of the cerebellar cortex. Purkinje cells showed irregularity in size and shape. Prominent perineuronal spaces were also observed. Some areas showed loss of Purkinje neurons leaving empty spaces. Granular layer showed areas of hemorrhage. Congested dilated blood vessel surrounded by a wide perivascular space can be seen. Moreover, some researchers found that Purkinje cells in the cerebellum were the most affected cell and there were signs of chromatolysis and gliosis (Shivarajashankara *et al*., 2002). Histological alterations in the cerebellum found in this study after NaF administration could be explained by increased oxidative stress. Alteration in the Purkinje cell layer after NaF exposure may cause changes in motor coordination and changes/loss of motor behavioral activities (Blaylock, 2007). It is established that Purkinje cells send inhibitory projections to the deep cerebellar nuclei, and they constitute the sole output of motor coordination in the cerebellar cortex (Shanthakumari, 2004). The changes in the molecular layer were thought to be secondary to changes in the Purkinje cells. As the degenerated Purkinje cells failed to establish contact with the molecular cells, this led to lack of normal synchronism between them that might minimize their regulatory role. This idea was supported by earlier postulations that assumed that several factors might be able to affect cerebellar interneurones and glial cell appearance (Trabelsi *et al*., 2001).

Quantified immunohistochemical assessments were conducted to elucidate mechanism(s) of NaF neurotoxicity. A significant up-regulation of iNOS expression, a marker of oxidative distress was detected in the NaF treated group. A significant increase in iNOS expression was reported in aged hippocampi, and in brains in cases of neurodegenerative disorders (Seham *et al*., 2008). It is hypothesized that iNOS generated NO could be one of the free radicals produced in cases of NaF neurotoxicity (Basha *et al*., 2011). However, iNOS plays a role in neurotransmission and neuromodulation. Inappropriate expression of iNOS appears to be deleterious as it is associated with seizures and brain damage (Koppula *et al*., 2012).

The elevated expression of iNOS was associated with a significant increase in the number of Bax-protein positive nerve cells and endothelial cells with decrease in Bcl-2 protein immunoreactive nerve cells and endothelial cells of NaF treated rats compared with control rats. Bcl-2 family is known to be regulators of cytochrome c release from the mitochondria. It is classified into antiapoptotic proteins such as Bcl-2 and Bcl-XL which reduce cytochrome release and pro-apoptotic proteins such as Bax and Bak that induce the release of cytochrome c and a loss of mitochondrial membrane potential (Howard *et al*., 2002). Thus, ratio of pro-apoptotic and anti-apoptotic Bcl-2 family may be a pivotal key to the release of cytochrome c from the mitochondria into the cytosol. Therefore, in the present study, the expression of Bcl-2 family was examined immunohistochemically to elucidate the involvement of Bcl-2 in NaF induced apoptosis. it was documented that NaF induce apoptosis in human gingival fibroblasts and renal tubular cells via activation of Bax expression and Bcl-2 suppression (Jung *et al*., 2006). It was stated that marked increase in the percentage of brain cell apoptosis occurred in rat offspring when exposed to high fluoride, low iodine or both treatments (Shivarajashankara, 2002). Previous investigator found that there is an intimate connection between the neurotoxicity of fluoride, aluminum and glutamate. He explained that fluoride produces injury to the central nervous system by several mechanisms. That of particular interest is the ability of fluoride to induce free radical generation and lipid peroxidation in the brain, especially in the hippocampus. In addition, fluoride enhances aluminum absorption from the gastrointestinal mucosa and across the blood-brain barrier. Of particular concern is the demonstration that fluoride readily forms a chemical complex with aluminum called aluminofluoride complex which act as an activator of G-proteins (Blaylock, 2004). Other researchers mentioned that fluoride ions in the presence of trace amounts of aluminum are apparently able to act with powerful pharmacological effects (Strunecká and Patočka, 1999). Other possible mechanisms of cell apoptosis induced by fluoride is through the following ways: firstly, fluoride is an effective activator of G-proteins and can probably induce a conformational change of G-proteins that regulate second messenger cAMP and Ca2+ thereby ultimately leading to cell apoptosis (Susa, 1999). Other possible mechanism of cell apoptosis is that fluoride is a chemically active ionized element. It can affect oxygen metabolism and induce the production of oxygen free radicals. At the same time, fluoride binds antioxidants (such as N-acetyl cysteine and glutathione) and other free-radical destroying enzymes and then it triggers oxidative stress, cell damage and even cell apoptosis (Anuradha *et al*., 2001). Additionally, fluoride can induce a change in the levels of expression of some apoptotic genes as proved by recent experimental study which stated that fluoride could induce up-regulation of nuclear factor Kappa B (NF-kB) and DNA neuronal damage (Zhang *et al*., 2008).

The expression of the inflammatory marker TNF-α was significantly increased in the NaF treated group compared with control. These results were supported by the results of others (Stawiarska-Pieta *et al*,. 2012) who reported that exposure to fluoride in excessive amounts can result in inflammatory reactions. It has been hypothesized that with fluoride exposure there should be an increase in various inflammatory mediators and chemokines.

Glial fibrillar acid protein (GFAP) immunostaining is the most commonly used method to examine the distribution of astrocytes and their response to neural degeneration or injury. The current work showed that the number of GFAP-positive astrocytes increased significantly in NaF treated group that revealed positive immunoreaction in the cytoplasm and processes of many astrocytes producing a brushy or starry appearance. The alterations in astrocyte number are possibly because of oxidative stress and free radical formation (Baydas *et al*., 2003). Also, these findings were in agreement with those of a study that deduced that mechanical and chemical insults to the brain stimulate the proliferation and hypertrophy of astrocytes with increased synthesis of intermediate glial filaments. This phenomenon is called reactive gliosis, which is a universal reaction of astrocytes with specific structural and functional changes (Baydas *et al*., 2006). During reactive gliosis, astrocytes secrete neurotoxic substances such as inflammatory cytokines and free radicals, which actively attack protein molecules within neurons, resulting in neuronal damage, and contribute toward the pathogenesis of neurodegenerative diseases (Bates, 2002).

In this study, a concomitant administration of NSO and NaF in the protected group could prevent degenerative changes and significantly reduce the fluoride-induced neurotoxicity, but not completely recovering the histopathological changes to normal. These findings are consistent with other reports (Ali and Blunden, 2003) that had demonstrated that nigella sativa is one of the most important antioxidants. Quantified immunohistochemical assessments were conducted to elucidate mechanism(s) of the potential protective effect of NSO. Our results have shown that NSO ameliorated the morphological and neuropathological changes

induced by NaF. Oxidative stress, apoptosis, and inflammation were reduced in the protected group. In addition, NSO treatment down-regulated astrogliosis.

A previous study (Hosseinzadeh *et al*., 2007) stated that N. sativa has a strong antioxidant action through its thymoquinone constituents that inhibit 5-lipoxygenase, which explains the different anti-inflammatory effects of these seeds. They added that, NSO showed potent anti-inflammatory effects on several inflammation based models through suppression of the inflammatory mediators prostaglandins and leukotriens. Thymoquinone could also act as a free radical and superoxide radical scavenger, improve mitochondrial function, inhibit lipid peroxidation process during ischemia-reperfusion injury in rat hippocampus and may also preserve the activity of various antioxidant enzymes such as catalase, glutathione peroxidase, and glutathione-S-transferase (Woo *et al*., 2012). It is well known that endogenous antioxidant enzymes are responsible for preventing and neutralizing the free radical-induced oxidative damage. The antioxidant enzymes, such as catalase, glutathione peroxidase, glutathione reductase, and glutathione-S-transferase, represent a major supportive team of defense against free radicals (Sung *et al*., 2000).

So, Administration of NSO restored the activities of these enzymes and decreased the generation of lipid peroxidation and protein carbonyl content in the cerebellum, frontal cerebral cortex, and hippocampus to normal levels. According to previous studies, NSO and thymoquinone were reported to prevent oxidative injury in a rat model of subarachnoid hemorrhage (Ersahin *et al* 2011) and during cerebral ischemia–reperfusion injury (Hosseinzadeha *et al*., 2007). Moreover, NSO and thymoquinone were found to prevent hippocampal neurodegeneration after chronic toluene exposure in rats (Cheng *et al*., 2001). In addition, N. sativa also has antimicrobial and antibacterial activities (Roy *et al*., 2006), immunomodulatory and anticancer properties (Mbarek *et al*, 2007). It was found that the defatted extract of nigella sativa increases glucose-induced insulin release in isolated rat pancreatic islets in a concentration-dependent manner (Rchid *et al*., 2004). Thus, N. sativa may represent a potential therapeutic modality in different clinical settings.

Accordingly, it was concluded that NaF adversely affected the brain by histological, immunohistochemical changes. These alterations are dangerous because of heavy human exposure to NaF in the environment. Concomitant administration of NSO as an excellent source of antioxidants and anti-inflammatory agent can protect against such hazardous effects.

REFERENCES

Ali, B.H and G. Blunden, 2003. Pharmacological and toxicological properties of nagila sativa. Phytother Res., 17: 299-305.

Anuradha, C.D., S. Kanno and S. Hirano, 2001. Oxidative damage to mitochondria is a preliminary step to caspase-3 activation in fluoride-induced apoptosis in HL-60 cells. Free Radic.Biol. Med., 31(3): 367-373.

Basha, P.M., P. Rai and S. Begum, 2011. Fluoride toxicity and status of serum thyroid hormones, brain histopathology, and learning memory in rats: a multigenerational assessment. Biol Trace Elem Res., 144(1–3): 1083-1094.

Bates, K.A., J. Fonte, T.A. Robertson, R.N. Martins and A.R. Harvey, 2002. Chronic gliosis triggers Alzheimer's disease-like processing of amyloid precursor protein. Neuroscience., 113: 785-796.

Baydas, G., M. Ozer, A. Yasar, S.T. Koz and M. Tuzcu, 2006. Melatonin prevents oxidative stress and inhibits reactive gliosis induced by hyperhomocysteinemia in rats. Biochem 71 (Suppl 1): S91-S95.

Baydas, G., R.J. Reiter, A. Yasar, M. Tuzcu, I. Akdemir and V.S. Nedzvetskii, 2003. Melatonin reduces glial reactivity in the hippocampus, cortex, and cerebellum of streptozotocin-induced diabetic rats. Free Radic Biol Med., 35: 797-804.

Blaylock, R.L., 2007. Fluoride neurotoxicity and excitotoxicity / microglial activation: Critical need for more research Fluoride., 40(2): 89-92.

Blaylock, R.L., 2004. Excitotoxicity: A possible central mechanism in fluoride neurotoxicity. Fluoride, 37(4): 301-314.

Cheng, J.T., I. Liu, T.C. Chi, T.F. Tzeng, F.H. Lu and C.J. Chang, 2001. Plasma glucose lowering effect of tramadol in streptozotocin-induced diabetic rats. Diabetes., 50: 2815-2821.

Chouhan, S and S.J. Flora, 2010. Arsenic and fluoride: two major ground water pollutants. Indian J Exp Biol., 48(7): 666-678.

Dabrowska, E., R. Letko and M. Balunowska, 2006. Effect of sodium fluoride on the morphological picture of the rat liver exposed to NaF in drinking water. Adv Med Sci., 51(Suppl 1): 91-95.

Dhar, V and M. Bhatnagar, 2009. Physiology and toxicity of fluoride. Indian J Dent Res., 20: 350-355.

El-Gharieb, M.A., T.A. El-Masry, A.M. Emara and M.A. Hashem, 2010. Potential hepatoprotective effects of vitamin E and Nigella sativa oil on hepatotoxicity induced by chronic exposure to malathion in human and male albino rats. Toxicol Environ Chem., 92: 395-412.

Ersahin, M., H.Z. Toklu, D. Akakin, M. Yuksel, B.C. Yegen and G. Sener, 2011. The effects of nigella sativa against oxidative injury in a rat model of subarachnoid hemorrhage. Acta Neurochir (Wien) 153: 333-341.

Feng, P., J.R. Wei and Z.G. Zhang, 2012. Influence of selenium and fluoride on blood antioxidant capacity of rats. Exp Toxicol Pathol., 64(6): 565-568.

Flora, S.J., M. Mittal, V. Pachauri and N.A. Dwivedi, 2012. Possible mechanism for combined arsenic and fluoride induced cellular and DNA damage in mice. Metallomics., 4: 78-90.

Graves, J.M., W. Daniell, F. James and P. Milgrom, 2009. Estimating fluoride exposure in rural communities: a case study in Western Washington. Wash State J Public Health Pract., 2: 22-31.

Graves, J.M., W. Daniell, F. James and P. Milgrom, 2009. Estimating fluoride exposure in rural communities: a case study in Western Washington. Wash State J Public Health Pract., 2: 22-31.

Hajhashemi, V., A. Ghannadi and H. Jafarabadi, 2004. Black cumin seed essential oil, as a potent analgesic and anti-inflammatory drug. Phytother Res., 18: 195-199.

Hosseinzadeh, H., S. Parvardeh, MN, Asl., H.R. Sadeghnia and T. Ziaee, 2007. Effect of thymoquinone and nigella sativa seeds oil on lipid peroxidation level during global cerebral ischemia-reperfusion injury in rat hippocampus. Phytomedicine., 14: 621-627.

Hosseinzadeha, H., S. Parvardeh, M. Nassiri, H.R. Sadeghnia and T. Ziaee, 2007. Effect of thymoquinone and nigella sativa seeds oil on lipid peroxidation level during global cerebral ischemia-reperfusion injury in rat hippocampus. Phytomedicine., 14: 621-627.

Howard, S., C. Bottino, S. Brooke, E. Cheng, R.G. Giffard and R. Sapolsky, 2002. Neuroprotective effects of bcl-2 overexpression in hippocampal cultures: Interactions with pathways of oxidative damage. J. Neurochem., 83(4): 914-923.

Jha, S.K., R.K. Singh, T. Damodaran, V.K. Mishra and D.K. Sharma, 2013. Fluoride in groundwater: toxicological exposure and remedies. J Toxicol Environ Health B Crit Rev., 16: 52-66.

Jung, J.Y., J.H., Park, Y.J., Jeong, K.H. Yang, N.K. Choi, S.H. Kim W.J. Kim, 2006. Involvement of Bcl-2 family and caspases cascade in sodium fluoride-induced apoptosis of human gingival fibroblasts. Korean J Physiol Pharmacol., 10(5): 289-295.

Kanter, M., O. Coskun, A. Korkmaz and S. Oter, 2004. Effects of Nigella sativa on oxidative stress and β-cell damage in streptozotocin-induced diabetic rats. Anat Rec A Discov Mol Cell Evol Biol., 279: 685-691.

Koppula, S., H. Kumar, I.S. Kim and D.K. Choi, 2012. Reactive oxygen species and inhibitors of inflammatory enzymes, NADPH oxidase, and iNOS in experimental models of Parkinson's disease. Mediators Inflamm., pp: 823-902.

Lu, Y., Z.R. Sun, L.N., Wu, X. Wang, W. Lu and S.S. Liu, 2000. Effect of high-fluoride water on intelligence in children. Fluoride., 33(2): 74-78.

Mbarek, L., H. Ait Mouse and N. Elabbadi, 2007. Anti-tumor properties of black seed (nigella sativa) extract. Braz J Med Biol Res., 40: 839-847.

Meddah, B., R. Ducroc, M. El Abbes Faouzi, B. Eto, L. Mahraoui and A. Benhaddou-Andaloussi, 2009. Nigella sativa inhibits intestinal glucose absorption and improves glucose tolerance in rats. J Ethnopharmacol., 121: 419-424.

Mullenix, P.J., P.K. Denbesten, A. Schunior and W.J. Kernan, 2005. Neurotoxicity of sodium fluoride in rats. Neurotoxicol Teratol., 17: 169-177.

Nagi, M.N., H.A. Almakki, M. Sayed-Ahmed and A.M. Al-Bekairi, 2010. Thymoquinone supplementation reverses acetaminophen-induced oxidative stress, nitric oxide production and energy decline in mice liver. Food Chem Toxicol., 48: 2361-2365.

Nolte, J., 2009. The human brain: an introduction to its functional neuroanatomy. 6th ed. Philadelphia: Lippincott Williams & Wilkins., pp: 570-573.

Northam, E.A. and F.J. Cameron, 2013. Understanding the diabetic brain: new technologies but old challenges. Diabetes, 62(2): 341-342

Rchid, H., H. Chevassus, R. Nmila, C. Guiral, P. Petit, M. Chokaïri and Y. Sauvaire, 2004. Nigella sativa seed extracts enhance glucose-induced insulin release from rat-isolated Langerhans islets. Fundam Clin Pharmacol, 18: 525-529.

Ricomini Filho, A.P., L.M. Tenuta, F.S. Fernandes, A.F. Calvo, S.C. Kusano and J.A.Cury, 2012. Fluoride concentration in the top-selling Brazilian toothpastes purchased at different regions. Braz Dent J 23: 45-48

Roy, J., D. Shaklega, P. Callery and J. Thomas, 2006. Chemical constituents and antimicrobial activity of a traditional herbal medicine containing garlic and black cumin. Afr J Tradit Complement Altern Med., 3: 1-7.

Saab, B.J., J. Georgiou, A. Nath, F.S. Lee, M. Wang and A. Michalon, 2009. NCS-1 in the dentate gyrus promotes exploration, synaptic plasticity, and rapid acquisition of spatial memory. Neuron., 63: 643-656.

Santoyo-Sanchez, M.P., M. Carmen Silva-Lucero, L. Arreola-Mendoza and O.C. Barbier, 2013. Effects of acute sodium fluoride exposure on kidney function, water homeostasis, and renal handling of calcium and inorganic phosphate. Biol Trace Elem Res., 152: 367-372.

Seham, A.E., R. Saadia and A. Rehab, 2008. Upregulation of the inducible nitric oxide synthase in rat hippocampus in a model of Alzheimer's disease: a possible mechanism of aluminium induced Alzheimer's. Egypt J Histol., 32: 173-180.

Shanthakumari, D., S. Srinivasalu and S. Subramanian, 2004. Effect of fluoride intoxication on lipidperoxidation and antioxidant status in experimental rats. Toxicol., 204: 219-228.

Shivarajashankara, Y.M., A.R. Shivashankara, P. Gopalakrishna, S. Rao and S. Hanumanth, 2002. Histological changes in the brain of young fluoride-intoxicated rats. Fluoride., 35(1): 12-21.

Sofroniew, M.V and H.V. Vinters, 2010. Astrocytes: biology and pathology. Acta Neuropathol., 119: 7-35.

Stawiarska-Pieta, B., B. Bielec, K. Birkner and E. Birkner, 2012. The influence of vitamin E and methionine on the activity of enzymes and the morphological picture of liver of rats intoxicated with sodium fluoride. Food Chem Toxicol., 50: 972-978.

Strunecká, A., 1999. J. Pharmacological and toxicological effects of aluminofluoride complexes. Fluoride., 32(4): 230-242.

Sung, H., J. Nah, S. Chun, H. Park, S.E. Yang and W.K. Min, 2000. In vivo antioxidant effect of green tea. Eur J Clin Nutr., 54: 527-529.

Susa, M., 1999. Heterotrimeric G proteins as fluoride targets in bone (Review). Int.J. Mol. Med., 3(2): 115-126.

Trabelsi, M., F. Guermazi and N. Zeghal, 2001. Effect of fluoride on thyroid function and cerebellar development in mice. Fluoride., 34:165-173.

Uz, E., O. Bayrak, E. Uz, A. Kaya, R. Bayrak and B. Uz, 2008. Nigella sativa oil for prevention of chronic cyclosporine nephrotoxicity: an experimental model. Am J Nephrol., 28: 517-522.

Vani, M.L and K.P., Reddy, 2000. Effects of fluoride accumulation on some enzymes of brain and gastrocnemius muscle of mice. Fluoride., 33(1): 17-26.

Varner, JA., K.F. Jensen, W. Horvath and R.L. Isaacson, 1998. Chronic administration of aluminum-fluoride or sodium fluoride to rats in drinking water: Alterations in neuronal and cerebrovascular integrity. Brain Res., 784(1-2): 284-298.

Venkataraman, P., K. Selvakumar, G. Krishnamoorthy, S. Muthusami, S. Prakash and J. Arunakaran, 2010. Effect of melatonin on PCB (Aroclor 1254) induced neuronal damage and changes in Cu/Zn superoxide dismutase and glutathione peroxidase-4 mRNA expression in cerebral cortex, cerebellum and hippocampus of adult rats. Neurosci Res., 66: 189-197.

Wang, J., Y. Ge, H. Ning and S. Wang, 2004. Effects of high fluoride and low iodine on biochemical indexes of the brain and learning-memory of offspring rats. Fluoride., 37(3): 201-208.

Woo, C.C., A.P. Kumar and G. Sethi., 2012. Thymoquinone: potential cure for inflammatory disorders and cancer. Biochem Pharmacol., 83: 443-451.

Xiang, Q., Y. Liang, L. Chen, C. Wang, B. Chen, X. Chen and M. Zhou, 2003. Effect of fluoride in drinking water on children's intelligence. Fluoride., 36(2): 84-94.

Zhang, C., C. Ren, H. Chen, R. Geng, H. Fan, H. Zhao, K. Guo and D. Geng, 2013. The analog of Ginkgo biloba extract 761 is a protective factor of cognitive impairment induced by chronic fluorosis. Biol Trace Elem Res., 153(1–3): 229-236

Zhang, M., A.Wang, T. Xia and P. He, 2008. Effects of fluoride on DNA damage, S-phase cell-cycle arrest and the expression of NF-κB in primary cultured rat hippocampal neurons. Toxicol. Lett., 179(1): 1-5.